Study of composite biomaterials containing antibacterial agents

PhD candidate: **Szabolcs-Zsolt Benyey**

***Scientific supervisor*: Prof. Dr. Viorica Simon**

CLUJ-NAPOCA, 2013

Table of Contents

Introduction

Calcium phosphate glasses or bioceramics are currently used in hard tissue replacement due to their excellent biocompatibility and osteoconductivity. Numerous studies show that bone-like apatite materials favour bone formation and regeneration, having optimal surface characteristics for osteoblast cells adherence, proliferation and differentiation [1]. Orthopaedic implants that are used for bone fixation or joint replacement have a very low actual current incidence of infection, if the procedures are performed by experienced surgeons (< 1 – 2%) [2], but the absolute number of these infections is anticipated to rise as the number of trauma victims and elderly patients requiring fixation or joint replacements increases [3].

Bacterial adherence onto the medical devices consist the first step in infection development and cannot be prevented entirely despite great efforts, as the use of strict hygienic protocols coupled with special sterile enclosures, laminar flow and intraoperative systemic antibiotic prophylaxis. This in turn leads to bacterial colonisation of the surface leading to formation of a microbial biofilm [4]. Bacterial microfilms represent a natural growth and survival strategy for bacteria being the preferred mode of existence over the planktonic form. The matured biofilm protects the bacteria within by several defence mechanisms, tied to the morphology of the biofilm, that provides a unique shelter for the bacteria to thrive in, resulting in thousand fold antibiotic resistance and the capacity to regenerate after an attack [5]. As a consequence of the biofilm, coupled with the compromised blood supply of a surgical wound that often is poorly approachable and has an inhibiting drug delivery effect to the site, the systemic antibiotic treatments have a reduced efficiency treating these infections [6]. The systemic treatment also has the negative aspect of side effects and toxicity for maintaining a high dose of antibiotic in the bloodstream above the therapeutic concentration. If however the antibiotic concentration falls in the sub inhibitory region, the development of resistance in infecting bacteria can develop. In some cases as the catheters and heart valves the materials can be tailored in such way as to minimise the adherence of proteins and subsequently bacteria as well. But in the orthopaedic field the attachment of the host tissue is desired, so the anti-adherent method cannot be used. Instead the local antibiotic release can be promising and effective procedure for delivering drugs at the implantation site in high delivery efficiency, continuous action, without the systemic side effects [7, 8].

Considering the all information introduced above the main purpose of this thesis was to develop antibiotics loaded bioactive glass as local drug delivery systems for possible applications in tissue engineering. The design of scaffolds which are able to regenerate bone with good

mechanical and functional properties is a promising alternative to the use of allografts, autografts, and metals. For this approach the silica based mezoporous bioactive materials were considered. They combine the bioactivity and high reactivity that leads to the formation of crystalline apatite-like phases similar to the inorganic component of bones. Moreover they present a high pore volume, narrow pore size distribution and large surface area that enable a good loading and release profile. The adsorption of drugs into mezoporous matrixes is determined by the pore size, but as the majority of drugs used in clinical practice are in the nanometre scale, they can easily be introduced into the pores of mezoporous matrices. It was shown that larger surface area increases the loading capacity of the matrix [9]

The structure of the thesis consists of six chapters, preceded by the presented introduction followed by general conclusions and list of tables and figures and references. The first chapter is a general consideration of the biomaterials, related infections and antibiotics that were used. The second chapter describes the synthesis methods used for the preparation of the bioactive glass samples, aerogels and microspheres. In the third chapter the experimental methods used in the thesis are presented in short, with the device descriptions and measuring parameters used. These first three chapters are left out from this summary.

The results of the thesis are presented in the last three chapters, selected results results will be presented in this summary also, in the order they were presented in the thesis. The fourth chapter presents the adsorption of proteins on the bioactive glass in different conditions by the help of X-ray Photoelectron spectroscopy and specific surface area analysis. The fifth chapter is divided in two parts and describes the tetracycline loading and release profile from microspheres and xerogels prepared via the sol-gel route close to the composition of 45S5Bioglass®. The last chapter is also structured in two parts: the first part introduces the xerogel characteristics, while the second part deals with the aerogel characteristics both regarding a sol-gel derived bioactive glass matrix with the composition 60%SiO_2 30%CaO 10%P_2O_5 (molar %). Both xerogel and aerogel samples are studied as potential local drug delivery systems. In this respect the loading and release profile of four different antibiotics were evaluated on both xerogel and aerogel. In addition, antimicrobial inhibition tests were also performed.

1 Bioactive glass surface- biological medium interactions

The first thing that biomaterials come in contact with when entering a biological environment are the biological fluids and consequently proteins from those fluids [10]. It is important to understand the interactions between the biological medium and the biomaterials. The

adsorption of proteins onto the surface determines the formation of biofilms, a process present in infections associated to medical implants, in dental caries, in environmental technologies [11]. One of the known influencing factors of protein adsorption is the ionic concentration of the liquid the protein is dissolved in [12], and implicitly the ionic strength. As a model protein horse methemoglobin is chosen, as it is mostly similar to human methemoglobin, but is far more common [13].

1.1 Sample preparation

The bioactive glass matrix used in this study was prepared using the sol-gel method (45% SiO_2, 24.5% Na_2O, 24.5% CaO 6% P_2O_5). The precursors used were tetraethoxysilane (TEOS), $Ca(NO_3)_2{\cdot}4H_2O$, $(NH_4)_2HPO_4$ and Na_2CO_3. After gelation the sample was aged at room temperature for 30 days, followed by a heat treatment at 310 ℃ for 1 hour. To further foster the protein adsorption, the bioactive glass surface was silanized with 3-aminopropyl-triethoxysilane (APTS) and afterwards treated with glutaraldehyde (GA) as protein coupling agent [14]. First the silanization process was carried out by immersing the glass in aqueous solution (0.45 mol/L) of 3-aminopropyl-triethoxysilane (APTS) for four hours. The pH of the solution was adjusted to 8 (using HCl 1M) and the temperature was kept at 80 ºC. After silanization the sample was washed with deionized water, than functionalized with glutaraldehyde (GA) [$CH_2(CH_2CHO)_2$] (1mol/L) for one hour, followed by rinsing in deionized water. For protein adsorption GA functionalized bioactive glass powder was immersed in horse methemoglobin solution for 4 hours. The horse methemoglobin solution was prepared with phosphate-buffered saline solution (pH 7.4, 2 mg/ml) using two different salt concentrations (10 mM NaCl and 500 mM NaCl). For both salt concentrations the amount of horse methemoglobin in the solution was of 25 mg/ml. To remove the unattached protein from the surface, the samples were washed three times in buffer solutions and then lyophilized.

1.2 Protein attachment investigation

1.2.1 Surface investigation (XPS)

To evaluate the adsorption of methemoglobin on the bioactive glass surface, XPS measurements were performed on the as prepared bioactive glass (BG), after functionalization with glutaraldehyde

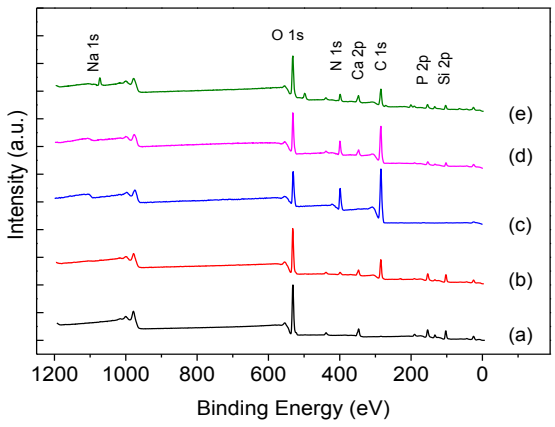

Figure 1-1: XPS survey spectra of BG (a), BG with GA (b), lyophilized horse methemoglobin (c), and BG-GA after immersion in protein solution with 10 mM NaCl (d) and 500 mM NaCl (e) respectively

(BG-GA) and after immersion in protein solution in low and high salt environment.

Using the survey spectra (Figure 1-1) the elemental composition of the top 10 nm of the samples can be precisely determined. The as prepared bioactive glass contains oxygen, silicon, calcium, phosphorus, sodium as expected from the preparation and also small amounts of carbon. The carbon appears on all surfaces exposed to air and can be used to calibrate the charge compensation of the samples [15]. The atomic concentration was calculated with CasaXPS software. From these data (Table 1-1) the evolution of the elements on the surface of the glass can be followed.

Table 1-1: Elemental composition of bioactive glass before and after surface modification with methemoglobin in 10 mM and in 500 mM NaCl buffer solutions

	Elemental composition (at %)								
Sample	**Si**	**Ca**	**P**	**Na**	**C**	**O**	**N**	**S**	**Cl**
BG	32.6	5	2.3	1.4	5.6	53	-	-	-
BG-GA	18	2.9	1.5	-	40.5	33.6	3.4	-	-
MetHb	-	-	-	-	64.8	18.4	16.7	0.1	-
BG-GA MetHb (10 mM	5.8	2.1	1	0.1	58.1	21.4	11.5	-	-
BG-GA MetHb (500 mM	10	3.5	3	2.6	38	33	7.7.	-	2

After silanization and GA treatment, the concentration of the carbon peak increases significantly, also a small nitrogen concentration appears. These are consequentially accompanied by a small decrease in the other components of the BG, meaning that a successful surface modification was achieved. Methemoglobin contains mostly carbon, oxygen and nitrogen (Table 1-1). The high concentration of carbon and nitrogen in both samples immersed in methemoglobin solution proves protein attachment, fact supported by the close C to N ratios in both samples compared to the lyophilized protein. Although from both salt concentrations protein attachment is evident, the effect is more pronounced for the buffer with lower salt content. Both carbon and nitrogen peaks appear almost twice in concentration compared to the samples obtained from high salt solution.

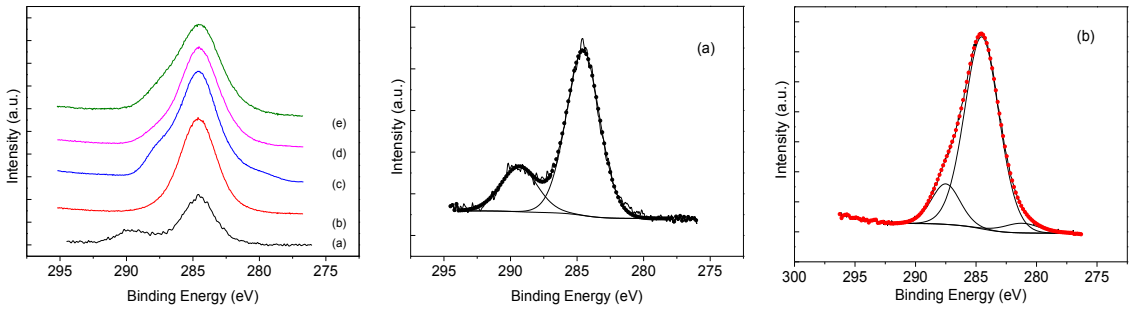

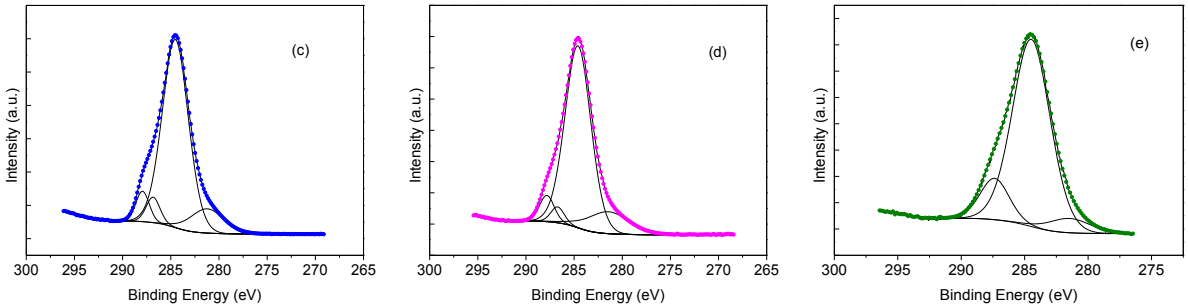

Figure 1-2: XPS C 1s high resolution spectra of BG (a), BG with GA (b), lyophilized horse methemoglobin (c), and of BG-GA after immersion in protein solution with 10 mM NaCl (d) and 500 mM NaCl (e) and their deconvolutions.

The high resolution spectra give information about the chemical states of the elements. The C 1s core-level spectra (Figure 1-2) recorded for protein loaded samples, compared to the bare sample evidence more intense and asymmetric peaks, confirming the presence of new types of carbon bonds [16, 17].

The deconvolution of the carbon core level spectra presents for the non-functionalized substrate one peak at 284.6 eV, corresponding to C-C and C-H bonds for the contamination from the air, as well as one at 289 eV representing the carbon from carbonate that still remains from the precursors in the bioactive glass. For the functionalized and protein covered samples the peak from the carbonates disappears. Additional components arise for the protein containing samples as well as in the protein itself: at 287.5 eV and 285.6 eV attributed to NH–CHR–CO and –C(=O)–NH2 respectively. Because of the charging effect the peaks have a shoulder at lower binding energies (around 281 eV).

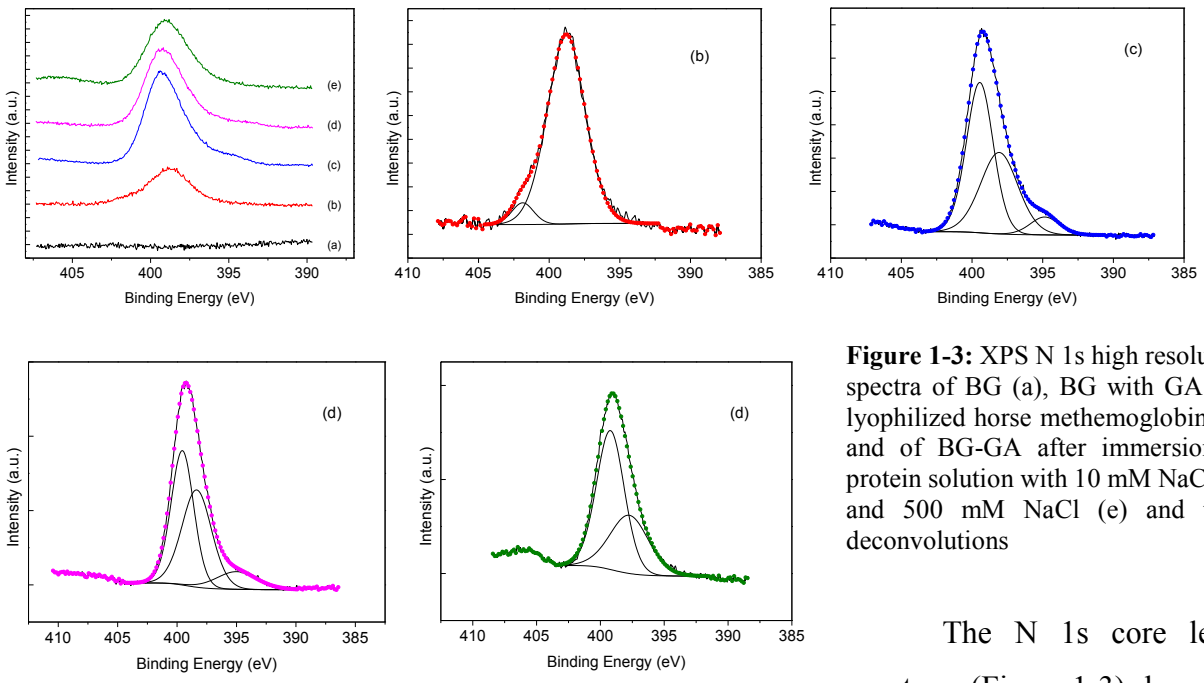

Figure 1-3: XPS N 1s high resolution spectra of BG (a), BG with GA (b), lyophilized horse methemoglobin (c), and of BG-GA after immersion in protein solution with 10 mM NaCl (d) and 500 mM NaCl (e) and their deconvolutions

The N 1s core level spectrum (Figure 1-3) shows no nitrogen present in the bare bioactive glass matrix. The N1s deconvolutions of the protein

containing samples show two main components around 400 eV and 397.8 eV, which can be attributed to nitrogen in organic matrixes, related to C-N bonds [18]. A smaller peak appears around 395 eV, which appears for protein itself and protein adsorbed from low salt solution.

1.2.2 Specific surface area analysis (BET)

The BET specific surface area and pore volumes are listed in Table 1-2. The surface area increased significantly after protein adsorption for both the samples prepared with low and high salt content. The pore volume decreases once the surface is loaded, this effect being even more pronounced for the sample immersed in low salt protein rich solution. Specific surface area and pore volume measurements suggest a larger amount of adsorbed protein in the case of low salt concentration, which expose a larger surface and enhance the surface porosity.

Sample	BET surface area (m^2g^{-1})	Pore volume (ml/g)
BG	98.6	0.46
BG-GA	106.0	0.38
BG GA MetHb (10 mM NaCl)	133.2	0.22
BG GA MetHb (500 mM NaCl)	121.7	0.23

Table 1-2: Specific surface area and pore volume recorded before and after methemoglobin adsorption

2 Study of bioactive glasses loaded with tetracycline

In order to diminish the bacteriological risk associated with an implant a local antibiotic release system is desired. Tetracycline is a broad-spectrum antibiotic [19] with an anti-inflammatory action which, in addition, exhibits anti-collagenase activity, inhibition of bone resorption, and the ability to promote attachment and proliferation of fibroblasts [20, 21]. Tetracycline is also an inhibitor of the activity of proteinases and hence can be used to treat or prevent diseases such as cancer metastasis, rheumatoid arthritis and osteomyelitis [22]

2.1 Bioactive glass preparation

The xerogels with a close composition to that of 45S5Bioglass® were prepared. Using the sol-gel method described above with starting materials (TEOS), $Ca(NO_3)_2{\cdot}4H_2O$, $(NH_4)_2{\cdot}HPO_4$ and Na_2CO_3 as SiO_2, CaO, P_2O_5 and Na_2O precursors to form the glass matrix to obtain the composition $45SiO_2{\cdot}24.5CaO{\cdot}24.5Na_2O{\cdot}6P_2O_5$ (mol %). After preparing the sol the drying was carried out in two different ways: by spray drying procedure, and by maturation followed by a heat treatment.

2.2 Spray dried microspheres

2.2.1 Microspheres preparation

To achieve spray dried microspheres loaded with tetracycline, Tetracycline (purchased from Sigma-Aldrich) dissolved in phosphate buffered saline (PBS) solution was mixed in the sol with 1mg/ml concentration, homogenised for half an hour. The achieved homogenous sol containing antibiotic was fed in the Buchi Mini Spray Dryer B-290.

2.2.2 Microspheres characterization

2.2.2.1 X-ray powered diffraction (XRD)

Figure 2-1 evidences the XRD patterns of spray dried bioactive glass, SD45 TCL and pure TCL. Since the tetracycline was incorporated inside the SD45-TCL samples the heat treatment was not performed in order to preserve the antibiotic structure. This lack of heat treatment can cause some precursors and solvents to remain trapped inside the materials as well as impurities in the form of $Ca_2Si_3O_2N_4$ and $NaNO_3$ as identified as the largest peak in both the tetracycline loaded and the simple bioglass located at 29° and 39°. The tetracycline loaded sample however shows some of the peaks of the antibiotic as well around 31°.

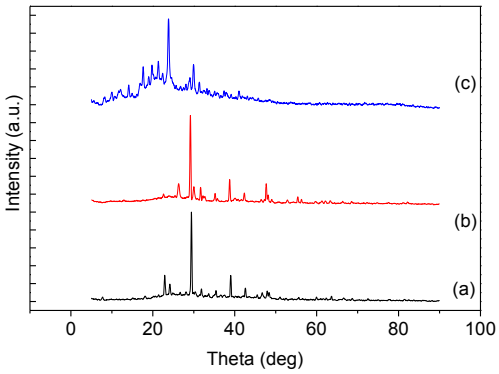

Figure 2-1: XRD diffractograms of spray dried bioactive glass (a), SD45 TCL (b), and pure TCL(c).

2.2.2.2 Morphological characterization (SEM)

The SEM micrograph taken from the sample (Figure 2-2) shows that after spray dying there were obtained microspheres with two size ranges, the majority of the microspheres are in the range of 5-10 µm, but there are also smaller particles in the range of 0.1-0.3 µm. The surface of the microspheres also looks smooth and they appear to be mostly intact.

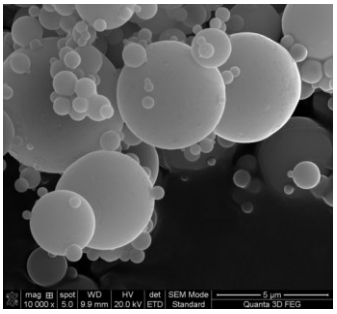

Figure 2-2: SEM image; magnification 10000 X

2.2.2.3 Particle size and specific surface area determination

The average diameter and size distribution of the bioactive glass microspheres are found to be around 10 µm, but a smaller distribution around 0.1 µm is also present (Figure 2-3). This finding correlates with the SEM images that show the same particle size, with two separate particle distributions. Studies made on bioactive glass microspheres in this size range show good bioactivity [23].

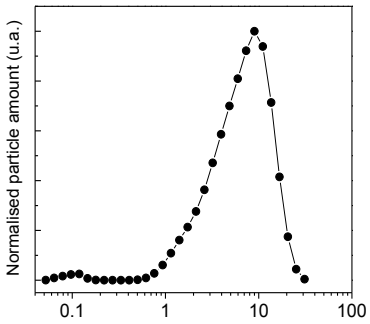

Figure 2-3: Particle size distribution of the microspheres**.**

The surface area of the material was determined using the BET nitrogen adsorption/desorption method. It was found that the microspheres have a small surface area around 4 m^2/g and no pore volume could have been measured, as the pore volume values were under the detection limit of the measuring device.

2.2.2.4 Zeta potential measurements

It has been demonstrated that negative zeta potential is beneficial for attachment and proliferation of bone cells [24, 25]. The value obtained by our measurements was -12.1 ± 1.5 mV at neutral pH (Figure 2-4). This puts it under the stability threshold, which means it is likely that the microspheres aggregate, fact evidenced by the SEM image as well (Figure 2-2).

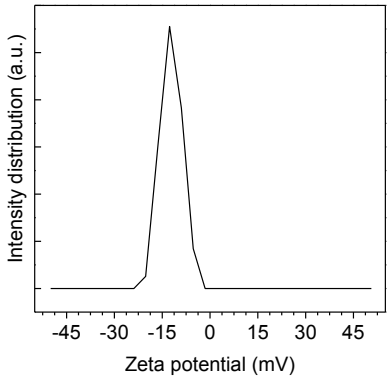

Figure 2-4: Zeta potential at neutral pH of microspheres

2.2.2.5 Surface investigation (XPS)

XPS measurements were carried out on the SD45 TCL and pure tetracycline as well. XPS measurement was performed on the bioactive glass microspheres after the release procedure described below to evaluate if there is still any antibiotic left on the microspheres surfaces.

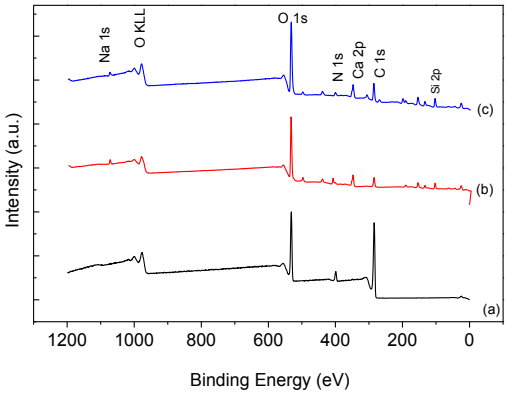

Figure 2-5: XPS survey spectra of (a) pure Tetracycline, (b) SD45-TCL before release and (c) SD45-TCL after release.

The atomic concentrations (Table 2-1) of over 20 % carbon, as well as nitrogen concentrations nearing pure tetracycline, clearly show the available antibiotic on the surface of the glass. The amount of carbon does not totally decrease even after the release study, which shows that part of the antibiotic is strongly attached to the glass matrix, and will be only released gradually with the bio absorption of the matrix. This is a desired effect and permits long term local treatment of the implantation sites.

Table 2-1: Surface chemical composition of pure tetracycline and of the BG-TCL microsphere before and after release

Sample	Elemental composition (at %)						
	C	N	O	Si	Ca	P	Na
TCL	72.9	5.4	21.6	-	-	-	-
BG-TCL	21.0	8.4	48.0	11.7	5.5	3.9	1.1
BG-TCL (after release)	26.4	3.4	43.7	15.3	4.9	5.0	0.9

2.2.3 Tetracycline release study

For delivery assays, spray dried glass (BG-TCL) (35 mg) was immersed in 5 ml simulated body fluid (SBF) prepared according to Kokubo protocol, pH 7.4, and kept at 37°C for 2, 5, 24 and 48 hours in Falcon tubes, with continuous stirring. After each period, the SBF solution was completely removed from the tube for analysis and replaced by another freshly prepared one.

2.2.3.1 Fluorescence and UV-Vis spectroscopy measurements

The SBF removed as described earlier was analysed by fluorescence and UV-Vis spectroscopy. The fluorescence and the UV-Vis spectra in the Figure 2-6 are not normalized or translated and so are in direct proportion with the released antibiotic concentrations over time. The release curve shows some exponential tendency at first, but nears linear in the later hours.

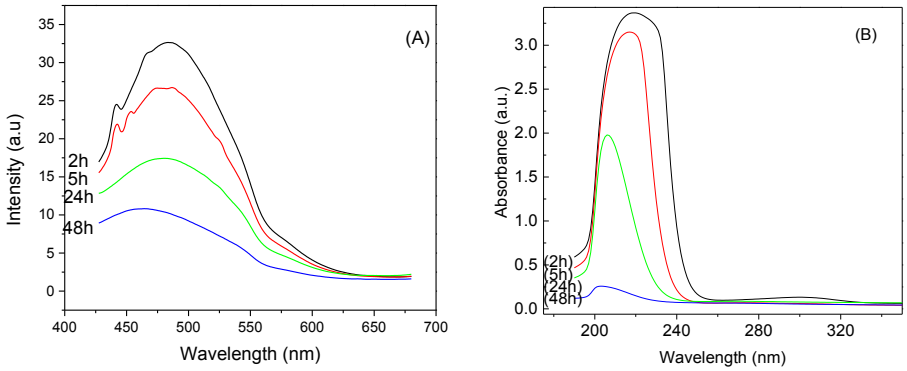

Figure 2-6: Fluorescence (A) and UV-Vis absorbance (B) spectra of tetracycline released from the spray dried bioactive glass after 2, 5, 24 and 48 hours

2.2.4 Antimicrobial inhibition

Antimicrobial inhibition tests were performed on methicillin resistant *S. aureus* strain UCLA 8076with a $5*10^5$ CFU/ml concentration. For this the SD45 TCL sample was diluted in ultrapure water at 75 mg/ml and spread on half the petri dish and the bacteria were spared on the

whole surface. After incubation at 36.8 ℃ for 24 hours, the dish was examined. As it can be observed in the Figure 2-7 the microspheres present some inhibitory effect where they are in larger concentrations, but fail to totally prevent bacterial formation on the microsphere treated side. Although the antibiotic concentration and dose released should be more effective in the inhibition this is not observed here. This can be caused by the initial heat while spraying that could damage the antibiotic structure leading to inactivation of the antibiotic. This damaged antibiotic could still appear in the spectroscopic studies, but will have reduced effect on the bacteria themselves.

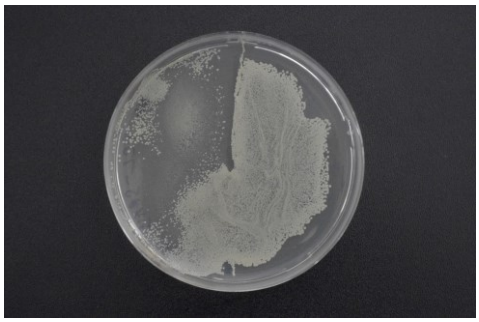

Figure 2-7: Antimicrobial inhibition results of the SD45 TCL

2.3 Sol-gel prepared bioactive glass

2.3.1 Sample preparation

The conventional drying procedure involved maturation of the sol at room temperature for 30 days followed by heat treatment at 310 °C for 1 hour. For further reference the sample obtained this way will be called SG45. The tetracycline loading of the SG45 was carried out by immersion in phosphate buffered saline (PBS) enriched with tetracycline (7 mg/ ml), and named SG45 TCL. The sample was analysed after immersion at 37°C for about 6 hours in order to establish the amount of adsorbed tetracycline. For the release study 35 mg of SG45 TCL was immersed in 10 ml SBF and kept there for 2,5, 24 and 48 hours. After each time period the SBF was collected and replaced with fresh one. The SG45 was treated according to the same procedure as the SG45 TCL.

2.3.2 Sample characterization.

2.3.2.1 Morphological characterization (SEM)

The SEM micrographs of the bioactive glass before and after antibiotic loading are presented in Figure 2-8. The image taken before loading shows a lamellar structure of the material and a porous character. After the loading procedure the surface gets a fuzzy appearance that could be associated to tetracycline adsorption [26].

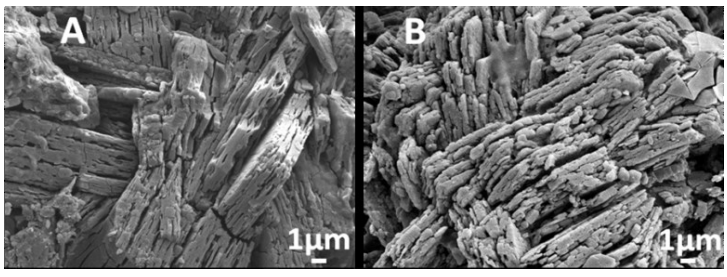

Figure 2-8: SEM images of SG45 before (A) and after (B) tetracycline loading

2.3.2.2 Surface investigation (XPS)

To evaluate the surface composition of the SG45 before and after loading XPS spectroscopy was used. With the help of this technique the composition of the top 10 nm of the studied samples can be determined.

XPS analysis of the survey spectra (**Error! Reference ource not found.**) recorded from pure tetracycline, and from tetracycline free and tetracycline loaded samples both before and after immersion in SBF aimed to determine the composition difference in the outermost layer. As it can be observed from Table 2-2, the carbon and nitrogen can be used as markers of tetracycline adsorption [24] because the two elements are not present in glass, even though carbon contamination is unavoidable and unpredictable in practice.

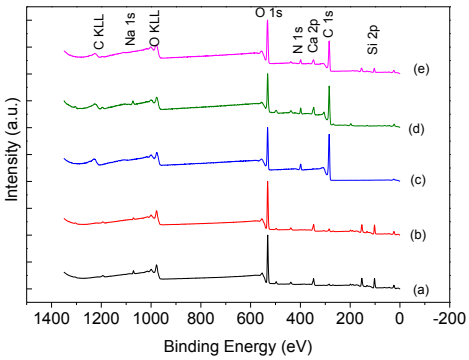

Figure 2-9: XPS survey spectra of SG45 (a), SG45 immersed in SBF (b), pure TCL (c), and SG45 TCL (d) and of SG45 TCL after 96 hr immersion in SBF for tetracycline release (e)

Table 2-2: Surface chemical composition before and after immersion of the SG45 in tetracycline (TCL) solution and after 96 hr immersion in SBF

Sample	Elemental composition (at %)						
	C	**N**	**O**	**Si**	**Ca**	**P**	**Na**
SG45	5.6	-	53	32.6	5	2.3	1.4
SG45/SBF	8.8	0.5	52.2	30.8	4.7	2.1	0.8
TCL	72.9	5.4	21.6	-	-	-	-
SG45/TCL	65.7	5.3	23.6	-	3.2	1	1.2
SG45 after TCL release	54.4	4.2	30.1	8.3	2.1	0.9	-

While carbon is present at the unloaded sample surface as contamination, the elemental analysis also indicates a remarkable increase of carbon content after incubation, content closed to the value obtained for tetracycline itself that proofs the tetracycline adsorption.

The N 1s, C1s and O 1s high resolution XPS spectra of (Figure 2-10) strengthen these results. One observes the high intensity of the nitrogen and carbon spectra (Figure 2-10-A (d),B(d)) recorded from the tetracycline loaded glass, in comparison to the tetracycline corresponding ones (Figure 2-10-A (c),B(c)). After immersion in tetracycline solution, the O 1s peak decreases in intensity and shifts to lower binding energy and the amount recorded is comparable to the value recorded for pure tetracycline, which is less rich in oxygen atoms.

After the release process the amounts of C, N slightly decreases while O increases together with silica which is revealed at the surface of the sample again. This means the tetracycline was

released in great amount, but significant quantity is still detected at the surface of the glass, which can be considered irreversibly bound.

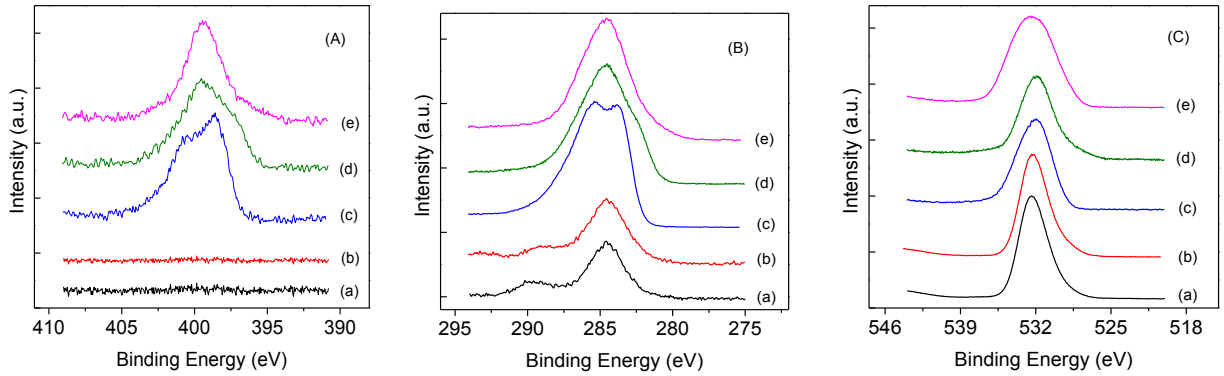

Figure 2-10: XPS high-resolution N 1s (A), C 1s (B), O 1s (C) spectra of SG45 (a), SG45 immersed in SBF (b), tetracycline (c), SG45 with tetracycline (d), and of SG45 after 96 hours immersion in SBF for tetracycline release (e)

2.3.2.3 Fourier transform infrared spectroscopy (FTIR)

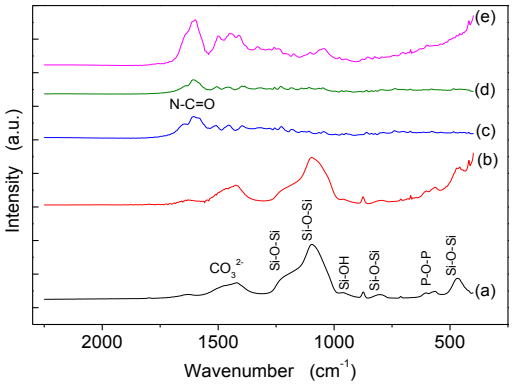

Figure 2-11: FT-IR spectra of SG45 (a), SG45 immersed in SBF (b), tetracycline (c), SG45 with tetracycline (d) and of SG45 after 96 hours immersion in SBF for tetracycline release (e).

Figure 2-11 presents FTIR spectra recorded from glass and tetracycline, as well as from glass immersed in SBF, tetracycline loaded glass and after 7 days glass immersion in SBF for tetracycline release. While the majority of the bands on the SG45 corresponds to the vibrations of high SiO_2 containing materials (1418 - 1470 cm^{-1} carbonate ;1200, 1090, 800, 466 cm^{-1} of Si-O-Si vibration [27]; 960 cm^{-1} Si-OH vibrations [28]; 606 and 564 cm^{-1} $PO4^{3-}$ [29]), the FTIR spectra of tetracycline and tetracycline loaded glass are very similar showing the same Amide I band around 1600 cm^{-1} [30] proof of tetracycline adsorption in great amount.

2.3.3 Antibiotic release study

2.3.3.1 Concentration evaluation (UV-Vis)

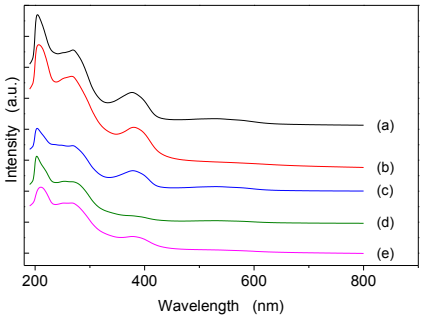

Figure 2-12: UV-Vis spectra recorded after 2 (a), 5 (b), 24 (c), 48 (d) and 96 (e) hours of tetracycline release from glass sample

Ultraviolet-visible absorption spectroscopy was used to estimate the amount of tetracycline released following the evolution of the absorption peaks of the tetracycline. The drug release is found to be fast for the initial 2 hours, gets slower for the next 5 and 24 and finally the release becomes constant for longer periods of time (Figure 2-12)

3 Study of SiCaP glasses loaded with different antibiotics

This part of the thesis presents the study of a bioactive glass matrix with the composition 60%SiO_2 30%CaO 10%P_2O_5 (molar %) loaded with different types of antibiotics. The antibiotics considered for this study were ampicillin, ciprofloxacin, streptomycin and tetracycline. These antibiotics were selected in order to evaluate their different affinity towards the bioactive glass matrix together with their release profile. These formulations are studied as potential drug delivery candidates to be used in bone repair implants.

3.1 Bioactive glass preparation

The precursors used for bioactive glass preparation (TEOS), Ca(NO3)2•4H2O and triethyl phosphate (TEP) to obtain a gel of 60%SiO_2 30%CaO 10%P_2O_5 (molar %) composition. Afterwards the gel was dried in two different ways to obtain xerogel and aerogel samples.

3.2 Xerogel bioactive glass

Part of the formed gel was dried at 110 ºC for couples of hours followed by heat treatment at 550 ºC for 2 hours. The heat treatment was performed (according to DTA measurements) in order to remove any unreacted organic component and to stabilize the glass network. The resulting glass was milled to a powder and then sieved to obtain a maximum grain size of 40 µm. This sample will be further called BG60.

3.2.1 Antibiotic loading

After a 24 hour SBF pre-treatment the bioactive glass was immersed into 10 gm/ml antibiotic containing PBS solution and kept four hours. After 4 hours the PBS solution was removed and kept for further analysis, and the bioactive glass was washed three times with fresh PBS to remove any unbound antibiotic. The samples loaded with antibiotics will further be named by the help of loaded antibiotic as: BG60 AMP, BG60 CIP, BG60 STR, and BG60 TCL.

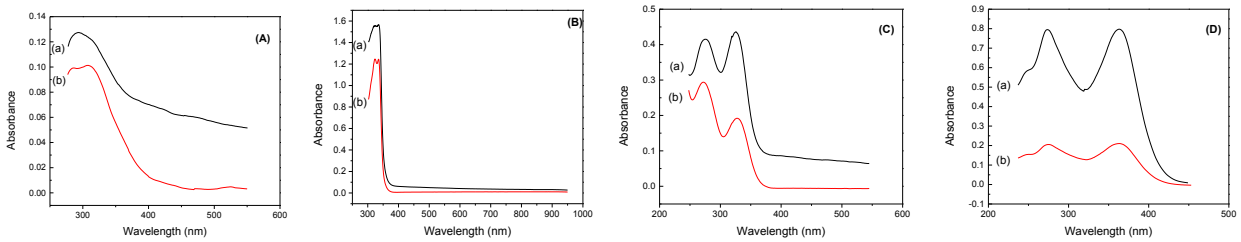

Figure 3-1: UV-Vis spectra of the initial antibiotic enriched PBS (a) and of the antibiotic enriched PBS after loading procedure (b) for ampicillin (A), ciprofloxacin (B), streptomycin (C), tetracycline (D).

To evidence the antibiotics loading into the porous bioactive glass-ceramic, the UV-Vis spectra of the initial PBS solutions with antibiotics were compared with the UV-Vis spectra of the solutions retrieved after 4 hours of immersion

The difference in intensities on all four samples (Figure 3-1) shows that part of the antibiotics is missing from the initial PBS solution indicating a successful attachment on the bioactive glass-ceramic surface, with a more pronounced effect for the samples containing tetracycline and less for the ampicillin loaded sample While tetracycline has a high affinity and capacity to form chemical bonds with Ca^{2+} ions from the bioactive matrix [31], the ampicillin has a reduced affinity towards bioactive glass surfaces due to charge effects, with the negatively charged ampicillin and BC repelling each other as reported by El-Fiqi et al. [32]. The streptomycin affinity towards this bioactive glass-ceramic matrix was found to be between the other two. Ciprofloxacin has also the capability to form Ca complex [33]. Although its affinity towards the bioactive glass matrix is not as high as the tetracycline's, it is a much more potent antibiotic which requires lower concentrations to achieve bacterial inhibition or bactericidal effect [34].

3.2.2 Sample characterization

3.2.2.1 Thermal analysis

To determine the heat treatment for the BG60 samples the thermal analysis was evaluated (Figure 3-2). The endothermic peak around 82℃ coupled with weight loss can be associated with the evaporation of the solvents from the material. The small exothermic peak with a weight loss can be associated to the decomposition of organic residues, while the large exothermic peak also with weight loss can be attributed to the decomposition of nitrates and dehydroxylation of the material. It can be noted that no significant change is observed after 550℃ in either TG or DTA curves, so for the treatment temperature of the samples this value was chosen.

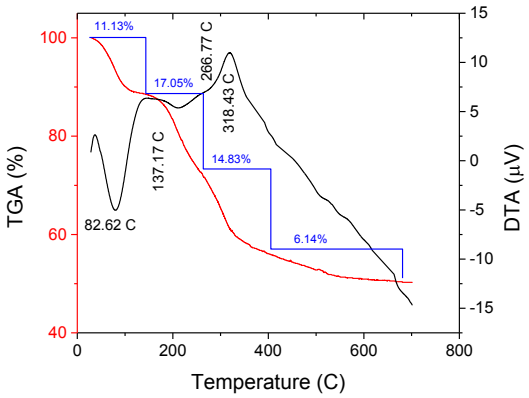

Figure 3-2: DTA/TG analysis of BG60 sample

3.2.2.2 Specific surface area analysis (BET)

The nitrogen adsorption/desorption studies (BET) before and after antibiotics loading (Table 3-1) show that the surface area of the loaded samples increases for all four composites. This phenomenon is expected and was also observed in protein adsorption studies described in the previous chapters. The increased surface area can be attributed to the extra surface roughness

provided by the attached antibiotic, which represents a proof of bioactive glass surface modification, following the antibiotic adsorption process.

Table 3-1: Specific surface area and mean pore volume of BG60 before and after antibiotics loading

	BG60	BG60 AMP	BG60 CIP	BG60 STR	BG60 TCL
Specific Surface (m^2/g)	52.63	67.65	67.52	69.85	67.98
Mean pore volume (ml/g)	0.11	0.35	0.33	0.29	0.33

3.2.2.3 Pore size distribution by NMR criporometry

For porosity evaluation by NMR crioporometry the bioactive glass sample was immersed in high purity water for more than 24 hours, as to permit the water to infiltrate the pores of the material. As the technique relies on the difference in phase transition temperatures the measurements are performed with a spin-echo sequence calibrated so that only the liquid will give signal. This allows the precise determination of the liquid quantity (Figure 3-4), which together with the measurement temperature values allow the phase transitions determination, and then calculate the pore size distribution. It was found that the pore radius have two distinct distributions, namely a dominant distribution with the mean radius located around 5.3 nm and a weakly pronounced distribution with the mean pore radius around 2 nm (Figure 3-3).

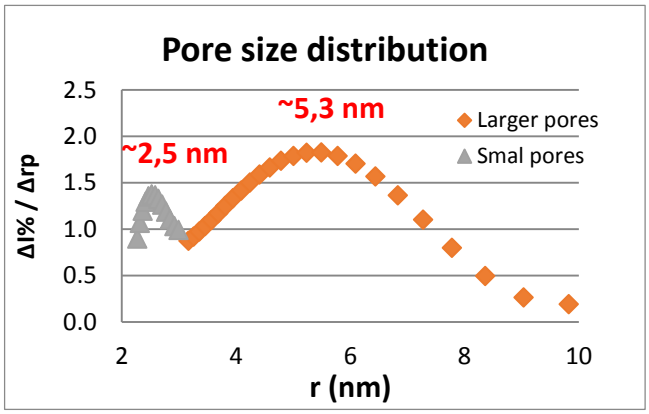

Figure 3-3: Pore size distribution of the bioactive glass samples calculated using NMR crioporometry; the two curves were fitted separately

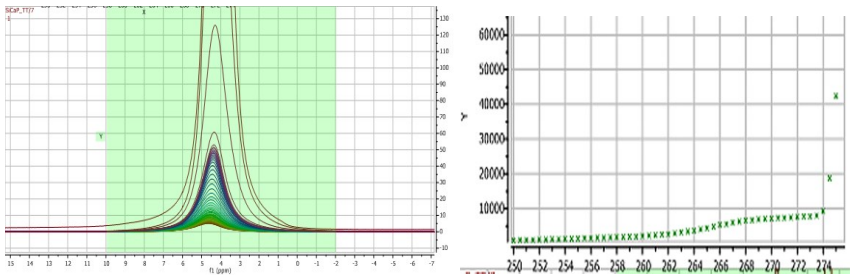

Figure 3-4: NMR spectra recorded for the crioporometry measurements (left) and the intensity of the peaks in relation to the temperatures at which the measurements were performed (right)

3.2.2.4 Zeta potential measurements

The zeta potential shows the charge difference between the stationary layer of fluid attached to the particles and the rest of the fluid. From biocompatibility perspective the negative zeta potential can be beneficial to the bone and tissue attachment to the material [25]. The Table 3-2 shows the zeta potential of the bioactive glass before and after antibiotic loading. As expected the BG60 surface is negatively charged. The antibiotics enhance the negative charge of the surface

especially the ampicillin which also has a negative charge. The only exception is the positively charged streptomycin that almost neutralizes the surface of the sample [35]. As a consequence of this we can assume that the streptomycin binding to the surface is aided by electrostatic interactions. The particle size for the powdered sample was in the micrometre range.

Table 3-2: Zeta potential of the BG60 before and after antibiotic loading

	Zeta potential (mV)	Average diameter (nm)
BG60	-21.53	973
BG60 AMP	-28	958
BG60 CIP	-27	964
BG60 STR	-0.175	868
BG60 TCL	-24.6	760

3.2.3 Bioactivity evaluation

To investigate the BG60 bioactivity, both the bare and the antibiotic loaded glasses were immersed in SBF for 14 days at 37℃, exchanging the SBF at a regular interval. After this time period of time, the samples were removed from the SBF, gently washed with ultra-pure water, dried at 37°C and evaluated for apatite like phase formations. The influence of antibiotics on glass bioactivity was also assessed.

3.2.3.1 X-ray powered diffraction (XRD) bioactivity study

The X-ray powder diffraction was used to assess the structure of the BG60 matrix and the fact that antibiotic loading does not decrease the bioactivity of the samples. The X-ray diffractogram (Figure 3-5 (a)) of the bare bioactive glass-ceramic sample obtained after heat treatment at 550 ºC for 2 hours show wollastonite ($CaSiO_3$) and apatite ($Ca_{10}(PO_4)_6(OH)_2$) like peaks at 29.1º and 32º , respectively [36, 37]

The size of the developed crystallites was estimated from the full width at half-maximum of the diffraction peaks using the Sherrer equation, and the average size was between 30 and 50 nm. The presence of both hydroxyapatite and wollsatonite is desirable for bioactive materials considered for scaffolds for bone tissue engineering [36-39].

To evidence the apatite like phases forming on the samples the XRD measurements recorded before and after SBF immersion are compared Figure 3-5. An increase in intensity of the peaks corresponding to the apatite like phases around 28°, 32° and 45° indicates a good bioactivity and apatite like phase forming capability of the prepared bioactive glass, even after loading with antibiotics.

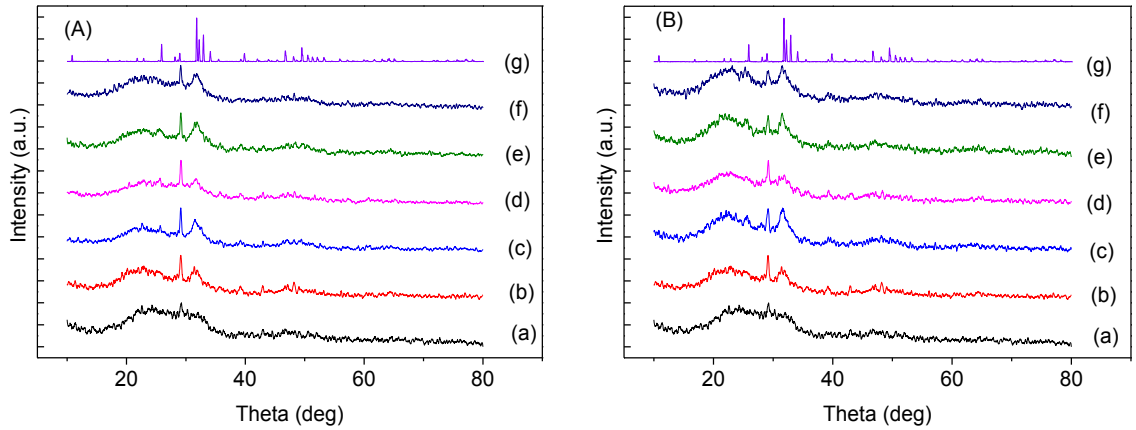

Figure 3-5: XRD patterns of BG60 (a), BG60 after 14 days of immersion in SBF (b), BG60 AMP (c), BG60 CIP (d), BG60 STR (e), BG60 SBF(f),Hydroxyapatite reference (g) – Before (A), and after SBF treatment(B)

3.2.3.2 SEM bioactivity assessment

By means of SEM we can evaluate the surface topography of the samples. They are mostly compact, homogenous looking, with porous microstructure. The pore size seems to be in the range of tens on nanometres, with nano sized surface roughness. SEM images show a change in the morphology of the samples following the SBF treatment. Figure 3-6 show the SEM micrographs of BG60 before and after SBF soaking for 14 days.

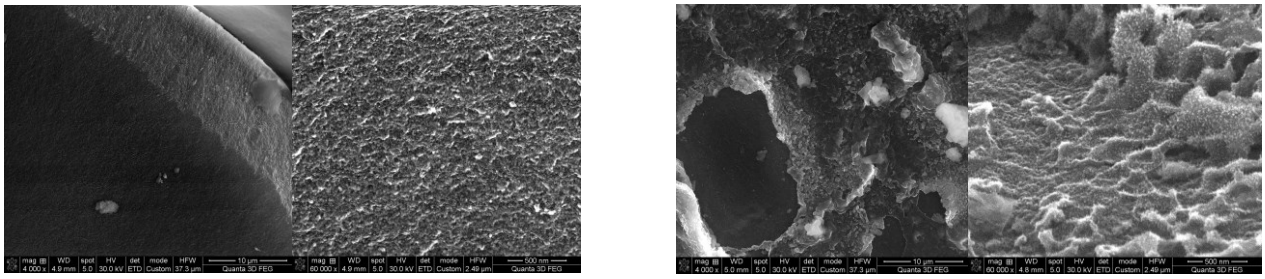

Figure 3-6: SEM images of the BG60 sample before (left) and after (right) SBF immersion recorded at different magnifications.

The characteristic apatite globular crystals are clearly visible. These changes can be attributed to the apatite like phases that form on the surface of the BG60 sample. The nanostructure changes as well fact evidenced by the numerous tiny crystals observed in the image with the highest magnification.

3.2.3.3 Fourier transform infrared spectroscopy (FTIR)

Figure 3-7 presents the FTIR spectra recorded for the bare bioactive glass matrix and for the matrix loaded with antibiotics before and after immersion in SBF for 14 days. It is observed a doublet around 589-600 cm^{-1}, increasing in intensity as a result of SBF immersion, attributed to the [PO4] unit vibrations corresponding to the crystalline hydroxyapatite [40]. The doublet is evident

also for the bare sample which strengths the previous statement according to the bioactive glass contain an appetite like phase even before SBF immersion. The FTIR results together with the XRD data prove that the loading of the bioactive glass matrixes with antibiotics will not hamper the bioactivity of the samples.

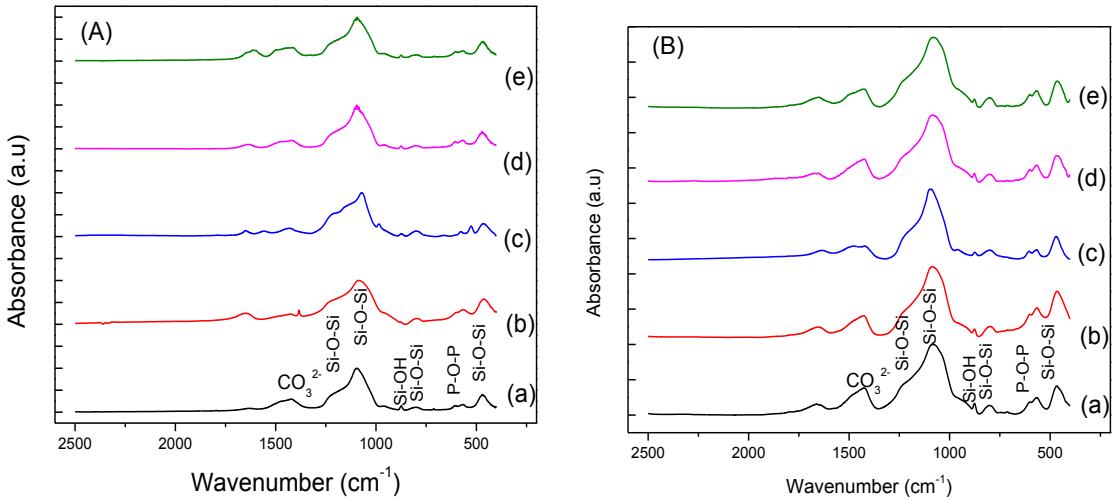

Figure 3-7: FTIR spectra of BG60 (a) BG60 AMP (b), BG60 CIP (c), BG60 STR (d) and BG60 TCL (e), before (A) and after (B) SBF immersion for 14 days.

3.2.4 Antibiotic release study

3.2.4.1 Concentration evaluation (NMR)

For the release profile evaluation a D_2O solution containing 0.1 mMol DSS was considered. 100 mg of bioactive glass loaded with each antibiotic was immersed in 700 µl of the as prepared D_2O solution. The D_2O solution was completely removed after 1, 2, 3, 5 and 24 hours respectively and replaced by freshly prepared one. The removed solutions were kept for analysis and loaded into NMR tubes. As reference, NMR spectra of 2 mg/ml of each antibiotic dissolved in D_2O solutions were also recorded (Figure 3-8)

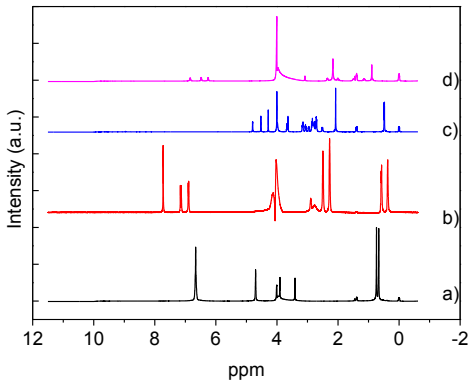

Figure 3-8: NMR Spectra of reference antibiotics with a 2mg/ml concentration, for ampicillin (a), ciprofloxacin (b), streptomycin (c) and tetracycline (d).

After phase correction and background deduction the prominent antibiotic peak integral was calculated relative to the DSS peak integral situated at 0 ppm. Because the values (Table 3-3) of the main integrated peaks corresponding to each antibiotic are relative values calibrated to the DSS, they become comparable and serve as a quantitative estimation. This calibration is necessary,

because otherwise the values can vary depending on the shim, tune or other factors that may influence the whole spectrum intensity.

Table 3-3: The concentration of antibiotics released in D2O determined from the NMR spectra

Release time	Antibiotic Concentrations (mg/ml)			
	BG60 AMP	BG60 CIP	BG60 STR	BG60 TCL
1h	0.036	0.057	0.024	0.667
2h	0.012	0.053	0.016	0.447
3h	0.004	0.047	0.011	0.397
5h	0.001	0.034	0.006	0.294
24h	0.001	0.019	0.012	0.420

The peaks used for integration and for concentration calculations are shown in Figure 3-9, and are normalised to the DSS peak to be a visual estimation of the released antibiotic amount. The antibiotic concentration calculated using this data then shows the release behaviour of the BG60 samples. The difference in the intensities of the peaks is proportional with the released concentrations.

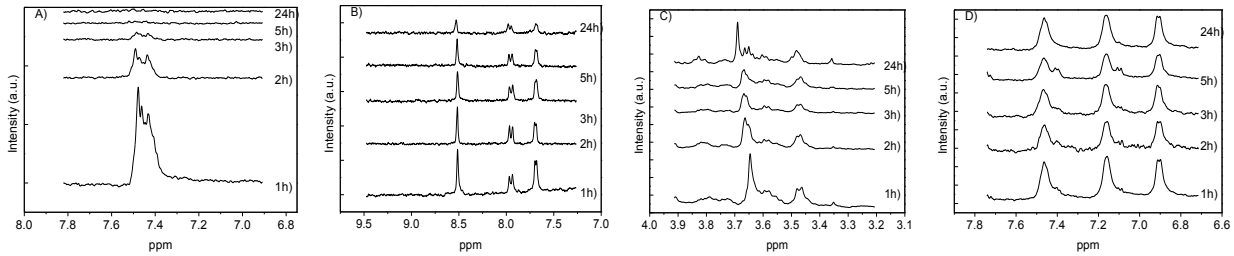

Figure 3-9: NMR peaks of the released antibiotic in D2O for BG60 AMP (A), BG60 CIP (B), BG60 STR (C),and BG60 TCL(D); the spectra were normalized to the DSS peaks**.**

3.2.4.2 Concentration evaluation (UV-Vis)

The antibiotics release profile in phosphate buffer solution (PBS) was also evaluated by UV-Vis spectroscopy using the same conditions as for the NMR. This data can also be correlated with the NMR release study; the only difference is the released medium's pH (7.4 in this case) which can induce some changes in the behaviour of the antibiotic release. As it can be observed from the Figure 3-10, the main aspects of the NMR release are found here as well. For ampicillin an initial burst release is followed by the low concentrations that are much closer to each other. This behaviour is strongly correlated with the weak binding capacity of ampicillin to this bioactive glass matrix. The same can be said for streptomycin: with an affinity slightly less than the tetracycline towards bioactive glass and the release curve close to exponential.

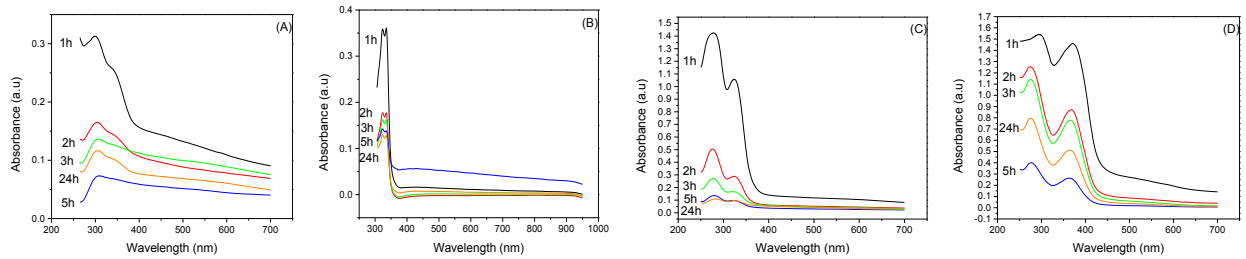

Figure 3-10: UV-Vis Spectra of the released antibiotic: ampicillin (A), ciprofloxacin (B), streptomycin (C) and tetracycline (D)

3.2.5 Antimicrobial inhibition

To test the effectiveness of the antibiotic loaded samples, antimicrobial inhibition tests were performed on both gram negative and gram positive bacteria.

3.2.5.1 Gram negative bacteria

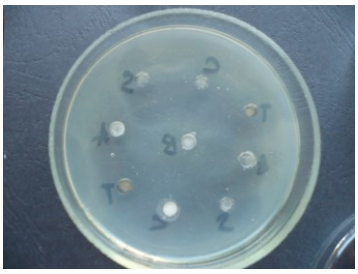

Figure 3-11: Antimicrobial inhibitory study on E-coli

To evaluate the effect on the gram negative bacteria the *E. coli* strain No. 25922 with a concentration of $3*10^8$ CFU/ml was considered. The antibiotic loaded samples were diluted in ultrapure distilled water and poured into 5 mm holes made in the agar, then the bacteria were spread on the whole surface of the Petri dish, and left 24 hour at 36.8℃ to form the bacterial colonies (Figure 3-11). The inhibition zones around the samples were evaluated and are displayed in Table 3-4.

Table 3-4: Antimicrobial inhibition zones around antibiotic loaded matrix, tested on E-coli (mm^2)

Plate	BG60 (mm^2)	BG60 AMP (mm^2)	BG60 CIP (mm^2)	BG 60 STR (mm^2)	BG 60 TCL (mm^2)
1	0	0	33	21	16
2	0	0	32	16	21
3	0	0	35	24	26
4	0	0	30	22	20
5	0	0	32	18	20
Average	0	0	32.4	20.2	20.6

Antimicrobial tests on the *E-coli* show a strong antimicrobial inhibition effect for tetracycline and streptomycin loaded samples, which indicate that the released antibiotics retain their efficacy after being released from the BG60, but the ciprofloxacin outperforms them all. This is a consequence of the strength of ciprofloxacin against the gram negative bacteria, and the release profile that permits the antibiotic to be present for a long duration of time. No inhibition effect for ampicillin loaded or blank bioactive glass matrix was evidenced. The lack of inhibitory effect in

case of the sample loaded with ampicillin could be associated with the small amount of ampicillin present on the surface of the bioactive glass matrix and the very fast release corresponding to this antibiotic.

3.2.5.2 Gram positive bacteria

For the gram positive bacteria methicillin resistant Staphylococcus aureus strain UCLA 8076 was utilized. The antibiotic loaded BG samples were first diluted in ultrapure water having a concentration of 70 mg/ml, then 100 µl of this diluted solution was applied to the half of a 90 mm Petri dish loaded with Mueller-Hinton agar. Then 100 µl of 10^7 CFU containing bacterial solution was spread across the whole dish, and left 24 hour at 36.8℃ to form the bacterial colonies. After 24 hours the Petri dishes were evaluated for antimicrobial activity. For control BG 60 was also spread across a petri dish in the same conditions described above, showing no inhibition (Figure 3-12).

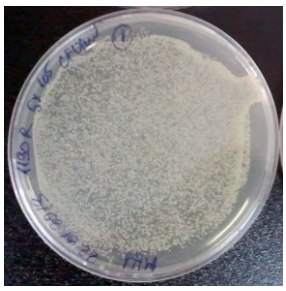

Figure 3-12: Antimicrobial inhibition tests on pure BG 60 performed on Staphylococcus aureus.

The Petri dishes were positioned so that the antibiotic loaded BG60 should cover the left side of the dish (Figure 3-13). The boundary was carved in with a sterile pipette into the agar to have a reference where the antibiotic treated surface ends and to estimate the inhibition zone from that boundary easier.

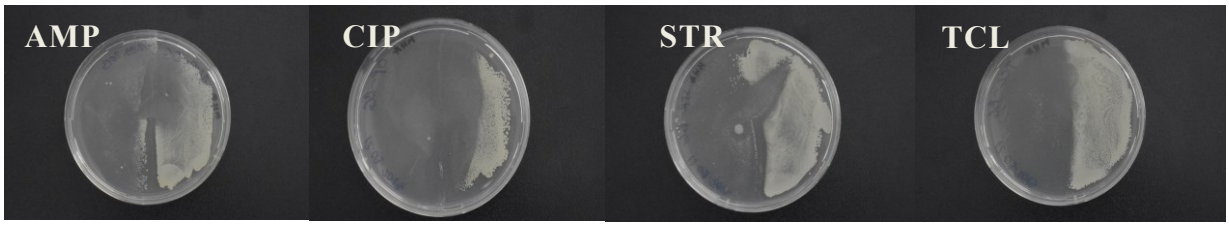

Figure 3-13: Antimicrobial tests performed on Staphylococcus aureus

As it can be observed the antibiotics have different antimicrobial inhibitory strength. Where the ampicillin had no effect on the E-coli, we observe some inhibition zones created by them on the Staphylococcus aureus cultures. This effect however fades in comparison to the other antibiotics. Where we can observe some colonies formed on the side coated with BG60 AMP, the BG60 CIP has a large inhibition zone over the boundary of the untreated surface as well. This effect can also be observed on the BG60 STR and BG60 TCL as well, although not in the same magnitude. These commonly used antibiotics should have a reduced effect on resistant bacterial strains, however the prolonged release and the large locally administered dose make them effective against these types of bacteria.

3.3 Aerogels

To obtain monolithic aerogel structures the gel prepared as described previously underwent a solvent exchange from water to ethanol and then to acetone, then dried supercritically using CO_2 (Figure 3-14). The obtained monoliths were then densified by a gradual heat treatment up to 1050°C.

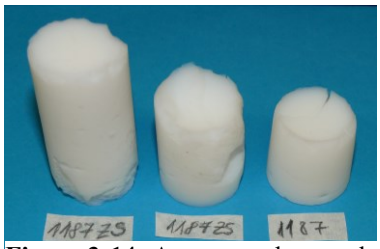

Figure 3-14: As prepared aerogels before heat treatment

3.3.1 Loading with antibiotics

The antibiotic loading procedure was similar to the one used on the xerogel. The samples were named after the antibiotic they were loaded with: Aero AMP for ampicillin, Aero CIP for ciprofloxacin, Aero STR for streptomycin and Aero TCL for tetracycline loaded matrix. To assess the antibiotics attachment on the aerogel the PBS collected after the loading procedure were compared with the original solutions using UV-Vis spectroscopy. The difference in intensity between the 10 mg/ml containing solution and the removed PBS shows that some of the antibiotic was loaded onto the aerogels. (Figure 3-15). The missing antibiotic from the removed samples demonstrates that the aerogels have bound some of the antibiotics that were dissolved in the PBS. The strongest difference in intensities can be observed on the tetracycline containing samples.

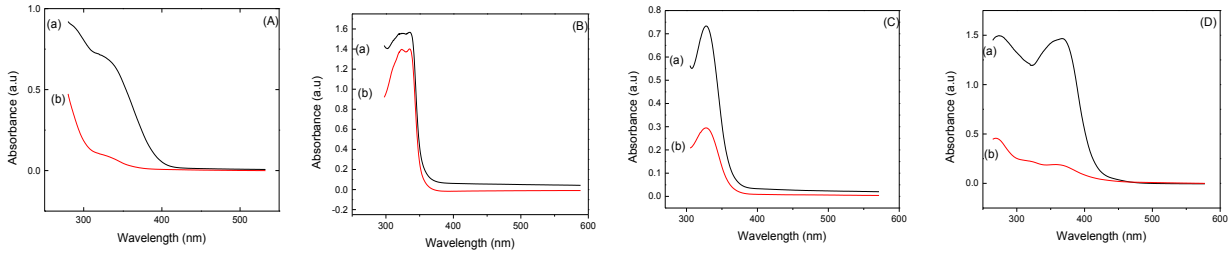

Figure 3-15: UV-Vis spectra of the initial antibiotic concentration (a) and the extracted antibiotic (b) for ampicillin (A), ciprofloxacin (B), streptomycin (C), tetracycline (D)

3.3.2 Sample characterization

3.3.2.1 Thermal analysis

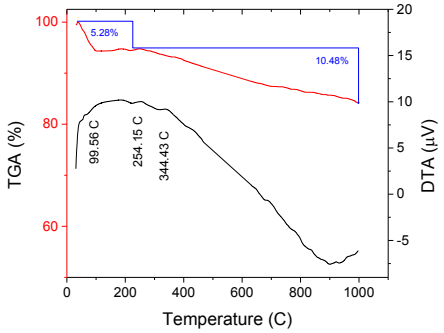

Figure 3-16: DTA/TG analysis of Aero 60 sample

The DTA thermographs of the sample shows no major events. The release of water absorbed at the surface of aerogel and the release of residual alcohol, occurring between 20 and 250°C. The small exothermic peaks around 250°C with a weight loss, can be attributed to oxidation of the alcoxy groups, while the one around 340°C to the elimination of a small amount of nitrate contamination.

The sample tends to be fairly stable with a total weight loss of around 15.76%. This stability is the consequence of the supercritical drying process which eliminates most of the unreacted precursors and solvents from the entire volume of the glass and is consistent with the thermo gravimetric studies on aerogel samples [41].

3.3.2.2 Specific surface area analysis (BET)

The recorded specific surface area and the mean pore volume for bare and antibiotics loaded aerogel are presented in Table 3-5. A relatively large specific surface area (205.5 m^2/g) and mean pore volume (0.64 ml/g) were recorded for the bare aerogel despite of a high treatment temperature. It can be seen that the surface area for the antibiotics loaded samples decreases significantly unlike to its counterpart xerogel sample. This behaviour can be associated with the SBF pre-treatment procedure that leads to an apatite like layer formation on the samples surface with a decreased porosity. As it can be observed in the SEM images as well after the SBF immersion for this sample (Figure 3-18), the apatite layer formation decreases surface roughness and subsequently specific surface area as well. Moreover, the size of the pores allows a penetration of the antibiotics inside the pores closing interconnected paths, leading to a further decrease in specific surface area and mean pore volume.

Table 3-5: BET Specific surface area of Aero60 before and after antibiotics loading

	Aero60	Aero60 AMP	Aero60 CIP	Aero60 STR	Aero60 TCL
Specific Surface Area (m^2/g)	205.56	133.79	144.56	141.69	146.73
Mean pore volume (ml/g)	0.64	0.52	0.54	0.51	0.56

3.3.3 Bioactivity evaluation

To evaluate the bioactivity of the samples and the effect of the antibiotics on the aerogel bioactivity, all the samples were introduced in SBF for 14 days and kept at 37℃. The SBF was changed twice a week with fresh one.

3.3.3.1 X-ray powered diffraction (XRD) bioactivity study

Figure 3-17 introduces the XRD patterns of heat treated aerogels, of the aerogel before and after 14 days of immersion in SBF together with the diffractograms corresponding to antibiotics loading aerogels, a hydroxyapatite XRD specific diffractogram was also included as reference.

The first thing noticeable in the samples loaded with antibiotics is a small peak around 32° that is typical for the apatite like phases formed as result of immersion in SBF for only one day as

a pre-treatment. On the bare aerogel matrix an apatite like peak appearing after soaking in SBF for 14 days can be observed, although the bioactivity of these samples should be somehow reduced due to the high treatment temperature, that is necessary to stabilize their structure. The antibiotic loaded samples also show this feature increased as compared to the bare sample. This tends to show that the antibiotic loading of the aerogels does not hinder their bioactivity.

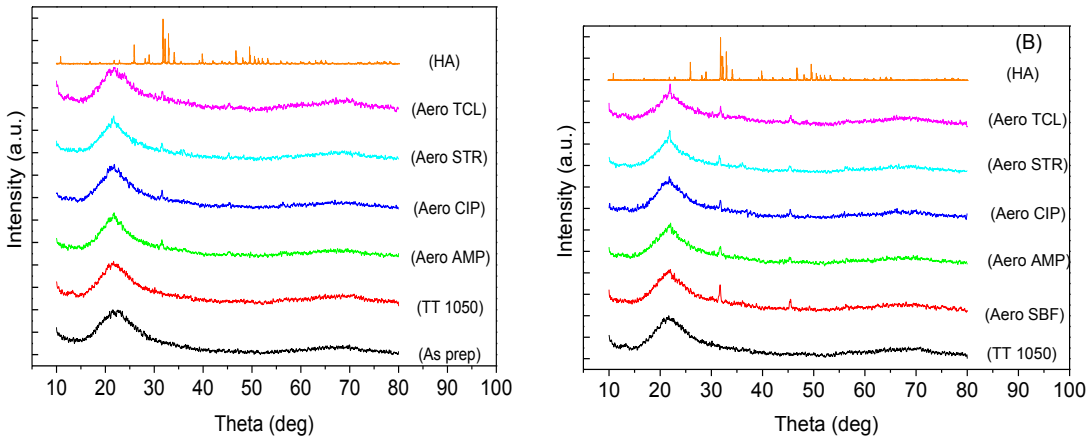

Figure 3-17: XRD patterns of aerogels before (A) and after SBF immersion (B)

3.3.3.2 SEM bioactivity assessment

To further assess the bioactivity of the aerogels their surface was investigated via SEM microscopy before and after SBF immersion. The aerogel samples present a porous interconnected morphology that strongly resembles the gel structure in its wet form. The surface of the materials looks homogenous and has mezoporous character. We can see that the surface is covered with highly interconnected, nanosized pores which results in large surface area of the material.

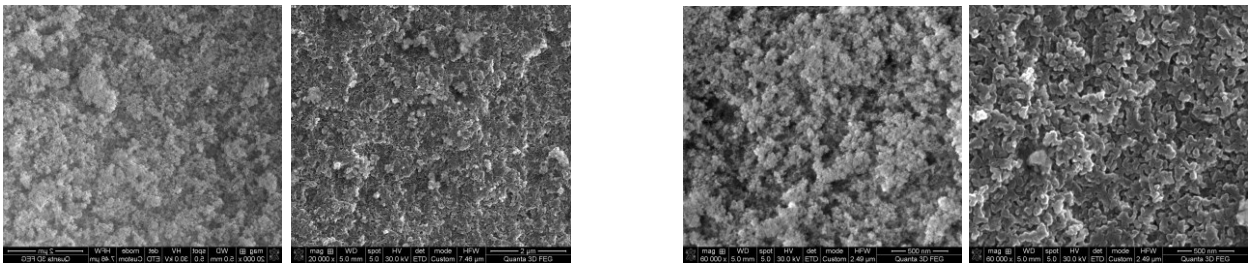

Figure 3-18: SEM images taken before (left) and after SBF immersion (right) at different magnifications.

The SEM images (Figure 3-18) show that after SBF immersion a layer has been deposited on the surface of the aerogels, which became smoother. This behaviour seems to have an impact also on the surface area of the aerogels which impact the antibiotic loading. The mesoporosity still remains but the nanofeatures seem to disappear from the sample surface.

3.3.4 Antibiotic release study

To evaluate the amount of antibiotic that can get released from the aerogel samples 100 mg of each of the antibiotic loaded samples was placed in 700 µl of D_2O marked with 0.1 mMol/l DSS and kept for 1,2,3,5 and 24 hours. After each time period the liquid was removed and replaced with a fresh one. The removed liquid was then analysed using NMR and UV-Vis spectroscopy.

3.3.4.1 Concentration evaluation (NMR)

By the help of NMR spectroscopy we can approximate the amount of antibiotics released within a certain time frame. To do this first the reference spectra of antibiotics was recorded (Figure 3-8). From these then a peak was chosen and the integrals relative to the DSS marker were calculated. For each different antibiotic then we got a release curve. The spectra for the different antibiotics were all cut so that they only show the selected peak and were all normalized to the DSS reference peak from 0 ppm (Figure 3-19).

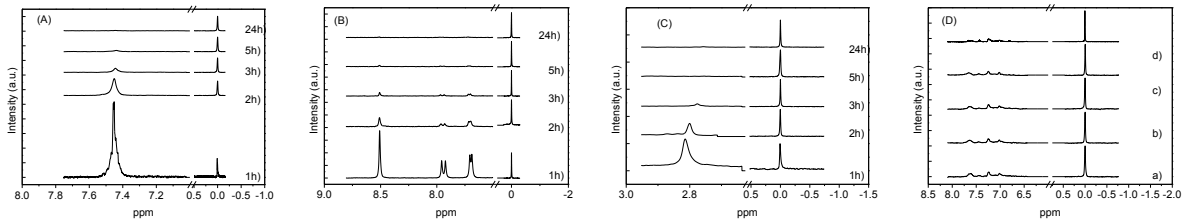

Figure 3-19: NMR antibiotic peaks for ampicillin (A), ciprofloxacin (B), streptomycin (C) and tetracycline (D). The peaks were normed to the DSS peak at 0 ppm.

From the antibiotic peak integrals we then calculated an approximate concentration of the released antibiotics. Because the same D_2O marked with DSS was used in all the release study, the DSS concentration is the same across the whole experiment, and the reference antibiotic concentrations were known. Taking this in account the antibiotic concentrations were approximated as the difference between the antibiotic peak integral and the DSS peak, which was calibrated at 1 for all the spectra (Table 3-6).

Table 3-6: Calculated antibiotic release concentrations

Release time	Antibiotic Concentrations represented in mg/ml			
	Aero AMP	Aero CIP	Aero STR	Aero TCL
1h	0.523	0.150	1.127	1.559
2h	0.212	0.011	0.193	1.462
3h	0.072	0.010	0.171	1.452
5h	0.028	0.009	0.110	1.398
24h	0.017	0.006	0.011	1.280

As it can be observed the antibiotic release is strongest in the first hour, followed by a steady decrease in concentrations over time. This was expected as the antibiotic concentration inside the aerogels decreases so does the released dose of antibiotics.

3.3.4.2 Concentration evaluation (UV-Vis)

To correlate with the NMR spectroscopy the release done for the UV-Vis spectroscopy mimicked the same starting conditions but using PBS as the solvent. The UV-Vis absorption spectra show a decrease in time of antibiotics concentration that can be correlated with the NMR results (Figure 3-20). This confirms the tetracycline linear release profile as well as the sharp decrease in intensity for the ciprofloxacin and ampicillin.

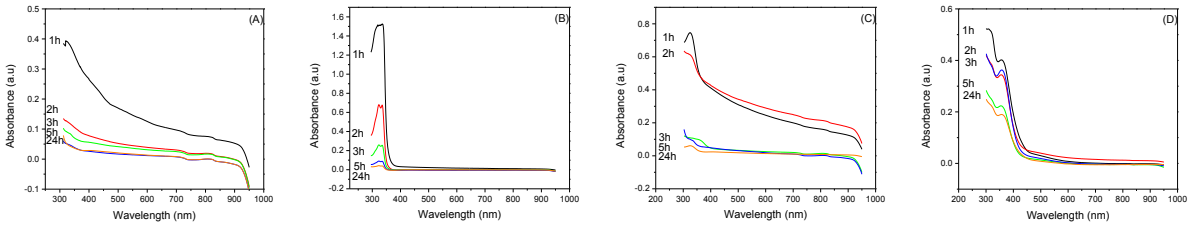

Figure 3-20: UV-Vis Spectra of the released antibiotic: ampicillin (A), ciprofloxacin (B), streptomycin (C) and tetracycline (D)

3.3.5 Antimicrobial inhibition

The antibiotic inhibition studies on the methicillin resistant staphylococcus aureus strain UCLA 8076 were carried out in the same conditions as for the BG 60. Control sample of Aero 60 coated petri dish was also treated in the routine described above, and shows no antimicrobial inhibition effect (Figure 3-21).

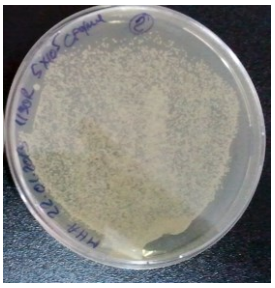

Figure 3-21: Antimicrobial inhibition tests on pure Aero 60 performed on Staphylococcus aureus

It can be observed that the ampicillin loaded aerogels have no inhibition effect on this bacterial strain (Figure 3-22). This can be due to the fact that ampicillin binds the weakest to the aerogels, and has a very fast release, effectively reducing the efficiency of the drug. On the other hand the antibiotics that can establish a stronger bound with the aerogel surface like ciprofloxacin or tetracycline, and have a more linear release, are more effective, also inhibiting a great part of the non-treated surface. Streptomycin is as seen before in between the lower performing ampicillin and the strong performing ciprofloxacin and tetracycline. It inhibits the bacterial formation on the whole surface on which it was spread but it is limited in the inhibition beyond the treated zone.

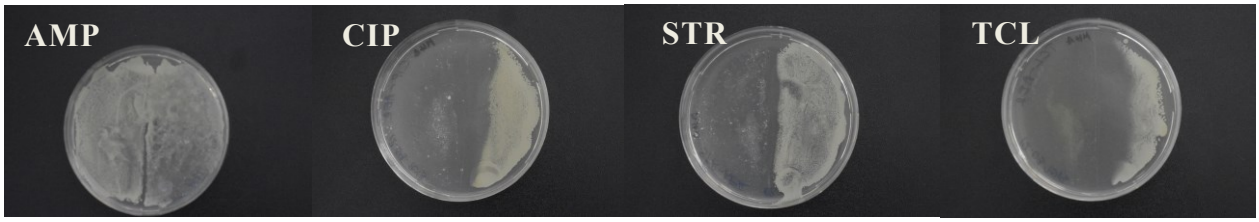

Figure 3-22: Antimicrobial inhibition study on Aero AMP, Aero CIP, Aero STR and Aero TCL **.**

.

General conclusions

- The sol-gel synthesis was used to create homogenous bioactive silicate materials with the composition $45SiO_2 \cdot 24.5CaO \cdot 24.5Na_2O \cdot 6P_2O_5$ (molar %).
- The protein adsorption study shows haemoglobin attachment for different ionic concentrations and surface treatments proving the receptiveness of the material towards the biological medium. Protein coupling agents and lower salt concentrations improved the adherence of the material, as evidenced by XPS spectroscopy. The surface area of the materials increases with the attachment of the protein as well.
- Incorporation of tetracycline into bioactive glass microspheres was achieved by spray drying procedure. This method led to obtaining the negatively charged microspheres with average diameter around 10 μm with a small surface area and smooth surface. Large dose of antibiotic incorporation is proven by XPS spectroscopy. The antibiotic release profile is almost linear over a prolonged time period. Inhibition tests present a poor antimicrobial activity despite the large antibiotic dose released, indicating possible damage of the antibiotic during spray-drying process.
- Tetracycline loading on the bioactive glass xerogel was analysed by XPS and FTIR spectroscopy and the antibiotic release profile was evaluated by UV-Vis spectroscopy. The ability of tetracycline to form chemical bounds with Ca^{2+} ions enabled great loading capacity, the antibiotic being still present on the glass surface even after 96 hours of release.

- Bioactive xerogel and aerogel samples were obtained by the sol-gel process with the composition $60\%SiO_2$ $30\%CaO$ $10\%P_2O_5$ (molar %), and loaded with different antibiotics.

I.

- The xerogel show wollastonite ($CaSiO_3$) and apatite ($Ca_{10}(PO_4)_6(OH)_2$) like phases evidenced by XRD, a large surface area and pore size around 10 nm.
- Antibiotic loading does not influence the xerogel bioactivity post SBF immersion, fact supported by the increase in the apatite like peak in XRD and the increase in the doublet around 589-600 cm^{-1} shown by FTIR spectra.
- The antibiotic release profile of the xerogel samples was evaluated by both NMR and UV-Vis spectroscopies.
- The antibiotics chosen proved different attachment characteristics and release profile:
    - Ampicillin evidenced weak attachment on the negatively charged bioactive glass due to its overall negative charge. This result in a really high initially burst, with the release of the almost entire amount of antibiotic in a short period time.
    - Ciprofloxacin has the capacity to chemically bind Ca and form complexes, resulting in a consistent loading of the antibiotic, a moderate initial burst followed by a more linear release profile.
    - Streptomycin is positively charged and its attachment is mediated by the electrostatic interactions. It presents a slow exponential release profile.
    - Tetracycline forms Ca complexes as well and attaches strongly to the material surface. It provides a consistent antibiotic dose in a constant release rate.
- Antimicrobial inhibition studies can be correlated with the antibiotics release behaviour. Ampicillin showed the weakest inhibition with no effect on gram negative bacteria and weak effect on gram positive bacteria. Streptomycin inhibits the whole surface where the antibiotic loaded sample has been applied, but no inhibition effect was evidenced apart from this area. Both ciprofloxacin and tetracycline show strong inhibition effect on gram positive bacteria, even outside the treated area, ciprofloxacin taking the lead in the inhibition of gram negative bacteria.

II.

- The aerogel sample characterization show that the material is highly homogenous, stable and vitreous even after heat treatments at 1050℃. It also possesses a larger surface area than the xerogel counterpart.
- The bioactivity of the aerogel samples does not suffer following the antibiotics loading, as apatite like phase is still evidenced after immersion in SBF by both XRD and FTIR.
- The antibiotic loading capacity of the aerogel samples its better comparing to the xerogel counterpart, due to the larger surface area of the material.

- The release profile of the antibiotics is similar to the xerogel counterpart. The only difference is the ciprofloxacin behaviour that has a strong initial burst followed by linear release behaviour.
- The antimicrobial inhibition shows no antimicrobial effect for the ampicillin. The streptomycin has only local inhibition effect as seen for the xerogel sample, and both ciprofloxacin and tetracycline inhibit a large region beyond the treated surface.

The antimicrobial bioactive materials presented in the thesis may be considered for bone defects restoration as a result of great bioactivity properties and promising response in terms of implant associated infections inhibition.

References

[1] J. Zhao, Y. Liu, W.B. Sun, H. Zhang, Amorphous calcium phosphate and its application in dentistry, Chemistry Central journal, 5 (2011) 40.

[2] W. Zimmerli, A. Trampuz, P.E. Ochsner, Prosthetic-joint infections, New England Journal of Medicine, 351 (2004) 1645-1654.

[3] T. Shunmugaperumal, Rationale for Biofilm Eradication from Modern Medical Devices, in: Biofilm Eradication and Prevention, John Wiley & Sons, Inc., 2010, pp. 36-72.

[4] P.S.P. Gorman, D.S. Jones, Antimicrobial biomaterials for medical devices, Microbiology, 74 (1996) 195-205.

[5] T. Shunmugaperumal, Biofilm Resistance–Tolerance to Conventional Antimicrobial Agents, in: Biofilm Eradication and Prevention, John Wiley & Sons, Inc., 2010, pp. 87-115.

[6] M. Miola, C. Vitale-Brovarone, C. Mattu, E. Verne, Antibiotic loading on bioactive glasses and glass-ceramics: An approach to surface modification, Journal of biomaterials applications, 28 (2012) 308-319.

[7] D. Arcos, M. Vallet-Regí, Bioceramics for drug delivery, Acta Materialia, 61 (2013) 890-911.

[8] L. Zhao, X. Yan, X. Zhou, L. Zhou, H. Wang, J. Tang, C. Yu, Mesoporous bioactive glasses for controlled drug release, Microporous and Mesoporous Materials, 109 (2008) 210-215.

[9] F. Balas, M. Manzano, P. Horcajada, M. Vallet-Regí, Confinement and Controlled Release of Bisphosphonates on Ordered Mesoporous Silica-Based Materials, Journal of the American Chemical Society, 128 (2006) 8116-8117.

[10] J. Xie, C. Riley, K. Chittur, Effect of albumin on brushite transformation to hydroxyapatite, Journal of biomedical materials research, 57 (2001) 357-365.

[11] I. Fenoglio, B. Fubini, E.M. Ghibaudi, F. Turci, Multiple aspects of the interaction of biomacromolecules with inorganic surfaces, Advanced drug delivery reviews, 63 (2011) 1186-1209.

[12] M. Vendruscolo, C.M. Dobson, Chemical biology: More charges against aggregation, Nature, 449 (2007) 555-555.

[13] J. Baldwin, The structure of human carbonmonoxy haemoglobin at 2.7 Å resolution, Journal of molecular biology, 136 (1980) 103-128.

[14] A. Dong, T.W. Randolph, J.F. Carpenter, Entrapping intermediates of thermal aggregation in alpha-helical proteins with low concentration of guanidine hydrochloride, The Journal of biological chemistry, 275 (2000) 27689-27693.

[15] R. Michel, S. Pasche, M. Textor, D.G. Castner, Influence of PEG architecture on protein adsorption and conformation, Langmuir : the ACS journal of surfaces and colloids, 21 (2005) 12327-12332.

[16] M.M. Browne, G.V. Lubarsky, M.R. Davidson, R.H. Bradley, Protein adsorption onto polystyrene surfaces studied by XPS and AFM, Surface Science, 553 (2004) 155-167.

[17] J. Serra, P. González, S. Liste, C. Serra, S. Chiussi, B. León, M. Pérez-Amor, H.O. Ylänen, M. Hupa, FTIR and XPS studies of bioactive silica based glasses, Journal of Non-Crystalline Solids, 332 (2003) 20-27.

[18] A.P. Serro, M.P. Gispert, M.C.L. Martins, P. Brogueira, R. Colaço, B. Saramago, Adsorption of albumin on prosthetic materials: Implication for tribological behavior, Journal of Biomedical Materials Research Part A, 78A (2006) 581-589.

[19] U.M. Wikesjö, P.J. Baker, L.A. Christlrsson, R.J. Genco, R.M. Lyall, S. Hic, R.M. Diflorio, V.P. Terranova, A biochemical approach to periodontal regeneration: tetracycline treatment conditions dentin surfaces, Journal of periodontal research, 21 (1986) 322-329.

[20] B.N. Vandekerckhove, M. Quirynen, D. van Steenberghe, The use of tetracycline-containing controlled-release fibers in the treatment of refractory periodontitis, Journal of periodontology, 68 (1997) 353-361.

[21] J. Goodson, M. Cugini, R. Kent, G. Armitage, C. Cobb, D. Fine, M. Fritz, E. Green, M. Imoberdorf, W. Killoy, Multicenter evaluation of tetracycline fiber therapy: II. Clinical response, Journal of periodontal research, 26 (1991) 371-379.

[22] M.G. Newman, K.S. Kornman, F.M. Doherty, A 6-month multi-center evaluation of adjunctive tetracycline fiber therapy used in conjunction with scaling and root planing in maintenance patients: clinical results, Journal of periodontology, 65 (1994) 685-691.

[23] B. Lei, X. Chen, Y. Wang, N. Zhao, Synthesis and in vitro bioactivity of novel mesoporous hollow bioactive glass microspheres, Materials Letters, 63 (2009) 1719-1721.

[24] E. Vanea, V. Simon, XPS study of protein adsorption onto nanocrystalline aluminosilicate microparticles, Applied Surface Science, 257 (2011) 2346-2352.

[25] J. Cooper, J. Hunt, The significance of zeta potential in osteogenesis, in: ANNUAL MEETING-SOCIETY FOR BIOMATERIALS IN CONJUNCTION WITH THE INTERNATIONAL BIOMATERIALS SYMPOSIUM, 2006, pp. 592.

[26] Â.L. Andrade, D. Manzi, R.Z. Domingues, Tetracycline and propolis incorporation and release by bioactive glassy compounds, Journal of non-crystalline solids, 352 (2006) 3502-3507.

[27] Â.L. Andrade, D. Manzi, R.Z. Domingues, Tetracycline and propolis incorporation and release by bioactive glassy compounds, Journal of Non-Crystalline Solids, 352 (2006) 3502-3507.

[28] H. Yoshino, K. Kamiya, H. Nasu, IR study on the structural evolution of sol-gel derived SiO< sub> 2</sub> gels in the early stage of conversion to glasses, Journal of non-crystalline solids, 126 (1990) 68-78.

[29] L.J. Jha, S.M. Best, J.C. Knowles, I. Rehman, J.D. Santos, W. Bonfield, Preparation and characterization of fluoride-substituted apatites, Journal of materials science. Materials in medicine, 8 (1997) 185-191.

[30] G. Falini, E. Foresti, I.G. Lesci, B. Lunelli, P. Sabatino, N. Roveri, Interaction of bovine serum albumin with chrysotile: spectroscopic and morphological studies, Chemistry (Weinheim an der Bergstrasse, Germany), 12 (2006) 1968-1974.

[31] P. Neuvonen, Interactions with the absorption of tetracyclines, Drugs, 11 (1976) 45-54.

[32] A. El-Fiqi, T.-H. Kim, M. Kim, M. Eltohamy, J.-E. Won, E.-J. Lee, H.-W. Kim, Capacity of mesoporous bioactive glass nanoparticles to deliver therapeutic molecules, Nanoscale, 4 (2012) 7475-7488.

[33] J. Al-Mustafa, Magnesium, calcium, and barium perchlorate complexes of ciprofloxacin and norfloxacin, Acta Chimica Slovenica, 49 (2002) 457-466.

[34] J.M. Andrews, Determination of minimum inhibitory concentrations, Journal of antimicrobial Chemotherapy, 48 (2001) 5-16.

[35] R. Brasseur, M. Carlier, G. Laurent, P. Claes, H. Vanderhaeghe, P.M. Tulkens, J.M. Ruysschaert, Interaction of streptomycin and streptomycylamine derivatives with negatively charged lipid layers: Correlation between binding, conformation of complexes and inhibition of lysosomal phospholipase activities, Biochemical pharmacology, 34 (1985) 1035-1047.

[36] M. Vallet-Regi, A.M. Romero, C.V. Ragel, R.Z. LeGeros, XRD, SEM-EDS, and FTIR studies of in vitro growth of an apatite-like layer on sol-gel glasses, Journal of biomedical materials research, 44 (1999) 416-421.

[37] R. Sreekanth Chakradhar, B. Nagabhushana, G. Chandrappa, K. Ramesh, J. Rao, Solution combustion derived nanocrystalline macroporous wollastonite ceramics, Materials chemistry and Physics, 95 (2006) 169-175.

[38] D.U. Tulyaganov, S. Agathopoulos, J.M. Ventura, M.A. Karakassides, O. Fabrichnaya, J.M.F. Ferreira, Synthesis of glass–ceramics in the CaO–MgO–SiO2 system with B2O3, P2O5, Na2O and CaF2 additives, Journal of the European Ceramic Society, 26 (2006) 1463-1471.

[39] X. Yang, L. Zhang, X. Chen, X. Sun, G. Yang, X. Guo, H. Yang, C. Gao, Z. Gou, Incorporation of B2O3 in CaO-SiO2-P2O5 bioactive glass system for improving strength of low-temperature co-fired porous glass ceramics, Journal of Non-Crystalline Solids, 358 (2012) 1171-1179.

[40] A. Vulpoi, C. Gruian, E. Vanea, L. Baia, S. Simon, H.J. Steinhoff, G. Göller, V. Simon, Bioactivity and protein attachment onto bioactive glasses containing silver nanoparticles, Journal of Biomedical Materials Research Part A, 100 (2012) 1179-1186.

[41] L. Kuchta, V. Fajnor, About the synthesis and thermal stability of SiO2-aerogel, Journal of thermal analysis, 46 (1996) 515-520.

Annex

Scientific papers:

1. Z. Benyey, E. Vanea, T. Simon, S. Cavalu, V. Simon, Tetracycline loading and release from bioactive glass microspheres, Studia Universitatis Physica, 56 (2011) 15-24.
2. E. Vanea, S. Cavalu, F. Bănică, Z. Benyey, G. Göller, V. Simon, Adsorption and Release Studies of Tetracycline from a Bioactive Glass, Studia Universitatis Chemia, 56 (2011) 239-247.
3. Z. Benyey, E. Vanea, C. Gruian, V. Simon, XPS Study of Methemoglobin Adsorption onto Glutaraldehyde Functionalized Bioactive Glass at Different Ionic Strengths, Studia Universitatis Physica, 57 (2012) 5-15.
4. Z. Benyey, E. Vanea, M. Tăuţan, M. Spinu, V. Simon, Synthesis and characterization of new bioceramic/antibiotic composites, Journal of Optoelectronics and Advanced Materials, in press 15 (2013).

National and international conferences:

1. Z. Benyey, E. Vanea, S. Cavalu, V. Simon, Sol-Gel prepared bioactive glass for administration of antibacterial agents, in: Advanced Spectroscopies on Biomedical and Nanostructured Systems, Cluj Napoca, 2011.
2. Vulpoi, Z. Benyey, H. Ylanen, V. Simon, Characterisation of silver nanoparticles containing bioglass coated polymer fabrics, in: Advanced Spectroscopies on Biomedical and Nanostructured Systems, Cluj Napoca, 2011.
3. Z. Benyey, M. Tăuţan, M. Niculae, E. Vanea, C. Gruian, M. Spinu, V. Simon, Antibiotics loading of glass matrix with possible use as bone scaffolds for the prevention of infections, in: 31st European Congress on Molecular Spectroscopy, Cluj Napoca, 2012.

4. Z. Benyey, M. Tăuţan, M. Niculae, E. Vanea, C. Gruian, M. Spinu, V. Simon, Preparation and characterization of antibiotic loaded bioactive glass matrixes for inhibition of biofilm formation at implant sites, in: 9th European Congress of Chemical Engineering, The Hague, 2013.